Astron. Astrophys. 357, 1073–1085 (2000)

ASTRONOMY AND ASTROPHYSICS

Nonlinear decay of phase-mixed Alfvén waves in the solar corona

Yu. Voitenko[1,2] **and M. Goossens**[1]

[1] Centre for Plasma Astrophysics, K.U.Leuven, Belgium (Yuriy.Voitenko@wis.kuleuven.ac.be)
[2] Main Astronomical Observatory, Kyiv, Ukraine

Received 22 November 1999 / Accepted 21 March 2000

Abstract. This paper presents an analytical investigation of the nonlinear interaction of phase-mixed Alfvén waves in the framework of two-fluid magnetohydrodynamics. It focuses on the parametric decay of the phase-mixed pump Alfvén wave into two daughter Alfvén waves. This parametric decay is a nonlinear phenomenon which does not occur in ideal MHD since it is induced by the combined action of finite wave amplitude and the non-zero gyroradius of the ions. In contrast to intuitive expectation, the effects of the non-zero gyroradius of the ions are already important at length scales that are substantially longer than the ion gyroradius. The parametric decay occurs for relatively small wave amplitude and is more efficient than collisional damping.

Key words: instabilities – Magnetohydrodynamics (MHD) – plasmas – waves – Sun: corona

1. Introduction

The physical mechanisms responsible for the heating of the solar corona still lack unambiguous identification. Resonant absorption and phase mixing (see Goossens 1994 and references therein) are two popular theories of Alfvén wave heating which involve spectral energy transfer towards small length-scales. Both are due to the transverse plasma inhomogeneity, typical for the corona. Phase mixing of Alfvén waves which leads to enhanced wave dissipation and consequent plasma heating, has been first proposed as a coronal heating mechanism by Heyvaerts & Priest (1983). Since then, phase mixing has been studied both for open and closed magnetic configurations (see recent papers by Ofman & Davila 1995**;** Hood et al. 1997a,b; Ruderman et al. 1998; De Moortel et al. 1999). The first conclusions on the asymptotic behaviour of the wave amplitudes with height, $\sim \exp\left(-z^3/z_c^3\right)$, or time, $\sim \exp\left(-t^3/t_d^3\right)$, have been recovered for the typical coronal conditions, when the length scale of the plasma inhomogeneity along the magnetic field lines, $L_\parallel$, is very large compared to that of the plasma inhomogeneity transverse to the magnetic field lines, $L_\perp$, $L_\parallel \gg L_\perp$ (e.g., Hood et al. 1997a). The only notable deviation from this behaviour was found by Ruderman et al. (1998), who presumed ad hoc that the scale height of wave damping is comparable to the vertical inhomogeneity scale.

Phase mixing of AWs induced by plasma flows has been studied by Ryutova & Habbal (1995). However, their results only apply to sub-Alfvénic flows, $v_0 \ll V_A$, as has been noted by Ruderman et al. (1999). Ruderman et al. (1999) relaxed the restriction of sub-Alfvénic flows and their investigation shows a good agreement between the linear analytical solutions and the nonlinear numerical simulations in the model of one-fluid nonlinear resistive MHD.

These results were obtained in the one-fluid MHD approximation. However, with the creation of short transverse length-scales in Alfvén waves, the Alfvén waves become essentially two-dimensional in the sense that they have long-wavelengths along the magnetic field and short-wavelengths across it. In this situation the ion polarization drift in the perpendicular direction creates a charge separation across $\mathbf{B}_0$, while field-aligned electron flows tend to cancel this charge separation, and thus the motions of the ions and electrons decouple from other. The finite temperature and/or electron inertia effects prevent complete charge cancellation, and a longitudinal wave electric field $\mathbf{E}_z \| \mathbf{B}_0$ arises. The presence of the longitudinal wave electric field, $\mathbf{E}_z \| \mathbf{B}_0$, and current, $\mathbf{j}_z \parallel \mathbf{B}_0$, bring about many new properties for Alfvén waves, including the effective interaction of waves with plasma particles (either via kinetic effects at Cherenkov resonance, or via collisions), as well as the nonlinear interaction with other modes and among Alfvén waves themselves. Since an adequate description of these effects requires kinetic plasma theory, these short-scale Alfvén waves are called kinetic Alfvén waves (KAWs).

Linear and nonlinear properties of KAWs have been extensively studied in the astrophysical and geophysical context. Examples are plasma heating (de Azevedo et al. 1994; Voitenko 1994), and current drive (Elfimov et al. 1996) in coronal loops in the solar atmosphere, instability of the interstellar plasma (Shukla et al. 1989), particles acceleration in galactic radio jets (Bodo & Ferrari 1982), impulsive energy release in solar flares (Voitenko 1996a,b, 1998c), wave instability (Voitenko et al. 1990 ; Hasegawa & Chen 1992) and plasma turbulence (Voitenko 1996c) in the Earth's magnetosphere, anomalous magnetic diffusion in coronal current layers

Send offprint requests to: Yuriy Voitenko

(Voitenko 1995). The nonlinear properties of KAWs are of great importance (Shukla & Stenflo 1995). In fusion devices, the efficiency of the energy exchange between waves and plasma particles caused by kinetic properties of KAWs has been proven recently both by theory and by experiment (Jaun et al. 1997).

It is thus surprising, that almost no attention has been paid to these properties of the KAWs created by the phase-mixing process in the non-uniform corona. Indeed, there are several papers studying the creation of short transverse length-scales in Alfvén waves and the eventual wave dissipation. There are also a few papers which concentrate on nonlinear effects in phase mixing (Nakariakov et al. 1997), and resonant absorption (Poedts & Goedbloed 1997). Ofman & Davila (1997) studied both the nonlinear excitation of sound waves and plasma heating by AWs in a nonuniform plasma in coronal holes. But these investigations have been carried out in the one-fluid MHD approximation, missing important properties of Alfvén waves with large transverse gradients developed by phase mixing.

The lack of interest in KAW in solar physics is due to an argument based on two characteristic transverse length scales, namely the Alfvén wave dissipation length scale l_d and the proton gyroradius ρ_i, with l_d being much longer than ρ_i. The fact that $\rho_i \ll l_d$ so that Alfvén waves are damped long before length scales of the order of ρ_i are set up by the phase mixed Alfvén waves leads to the intuitive conclusion that non-zero proton gyroradius effects are unimportant for Alfvén waves. However, this intuitive conclusion can be erroneous.

In the present article we shall show that the finite (ion) Larmor radius (FLR) effects in Alfvén waves can come into play at length scales which are much longer than both ρ_i and l_d. In this paper we study the parametric decay of a phase-mixed AW into two daughter AWs, induced by the combined action of the finite wave amplitude and FLR effects. This is an important nonlinear process which significantly modifies the wave spectral dynamics of phase mixing. So we are not concerned with the mechanisms that create phase mixed Alfvén waves. Instead, we try to find out how the nonlinearity induced by phase mixing affects the wave spectral dynamics.

A significant input of energy into a plasma, as observed in the solar corona, can only be achieved if the launched waves have sufficiently large amplitudes. E. g., AWs can balance the energy loss from the loop structures of active regions and from coronal holes, if the wave magnetic field amounts to 1-5% of the background magnetic field B_0. Nonlinear effects become important for waves of such amplitudes, and the ability of the waves to participate in different kinds of nonlinear interaction have to be examined.

It is well known that ideal MHD Alfvén waves cannot interact among themselves. Nonlinear coupling of AWs with other waves has been studied for a parallel-propagating pump wave (Galeev & Sagdeev 1979; Goldstein 1978; Viñas & Goldstein 1991; Jayanti & Hollweg 1993; Ghosh et al. 1993). In particular, the parametric decay into oblique waves was studied analytically (Viñas & Goldstein 1991) and numerically (Ghosh et al. 1993), and the consequent development of anisotropic turbulent cascade has been observed in numerical simulations (Ghosh & Goldstein 1994). In the Discussion we shall go into the details of how our approach differs from that used in the papers cited above. Here it suffices to note that we start with spectral anisotropy (due to phase mixing) which then initiates the nonlinear spectral dynamics. The papers cited above consider the reverse sequence.

We show that the influence of the three-wave nonlinear interaction becomes important with the creation of small transverse length-scales in the phase-mixed Alfvén waves, and can significantly change the picture of the phase mixing in the corona. In order to describe this process, we have to take into account that the motions of the electrons and the ions in AWs become decoupled from each another at small length-scales, and that the wave dynamics can be adequately described by kinetic theory. The nonlinear kinetic theory of KAWs, including nonlinear three-wave resonant interaction and linear Cherenkov wave-particle resonant interactions, has been developed by Voitenko (1998a). The collisional effects can be self-consistently taken into account in this theory by including collisional integrals into the Vlasov equations.

However, when we consider the low-frequency part of the Alfvén wave spectrum in the solar corona, $\omega \lesssim 1 - 100\ \mathrm{s}^{-1}$, we note that irrespectively of the KAW wavelengths, the linear kinetic damping is weaker than the collisional dissipation in this frequency range (Voitenko & Goossens 2000). Neglecting kinetic wave-particle interaction, some properties of these waves, such as thermal wave dispersion, collisional dissipation, and nonlinear three-wave interaction, can be described in the framework of the much simpler two-fluid MHD model. As is pointed out in the Discussion, the high-frequency AWs with $\omega \gtrsim 1 - 100\ \mathrm{s}^{-1}$, which can be excited by the chromospheric magnetic activity (Axford & McKenzie 1992), can be also approximately described by two-fluid MHD with kinetic effects taken from kinetic theory.

The paper is arranged as follows. The basic equations are presented in Sect. 2. The second-order two-fluid MHD theory of the nonlinear plasma motions in short-scale Alfvén waves is developed, and the Alfvén wave eigenmode equation is derived in Sect. 3. The collisional (linear) damping of short-scale Alfvén waves results in the same asymptotic behaviour of the wave amplitude as was found by Heyvaerts & Priest (1983) (Sect. 4). The parametric decay of a pump oblique AW into two daughter oblique AWs is considered in Sect. 5, and the results are applied to a phase-mixed AW propagating upward in the solar corona in Sects. 6 and 7. We discuss possible consequences of this process in the solar corona in Sect. 8 and present our conclusions in the last section, Sect. 9.

2. Basic equations

The wave electromagnetic fields obey Maxwell's equations

$$\nabla \times \mathbf{B} = \frac{4\pi}{c}\mathbf{j} + \frac{1}{c}\frac{\partial \mathbf{E}}{\partial t}, \tag{1}$$

$$\nabla \times \mathbf{E} = -\frac{1}{c}\frac{\partial \mathbf{B}}{\partial t}, \tag{2}$$

$$\nabla \cdot \mathbf{E} = 4\pi Q, \tag{3}$$

where the current density, $\mathbf{j}=\sum_s q_s n_s \mathbf{v}_s$, and the charge density, $Q=\sum_s q_s n_s$, have to be calculated using a suitable mathematical model of the plasma. The most popular models are based on the ideal MHD equations, the two-fluid MHD equations, and kinetic Vlasov equations.

As discussed in the Introduction, we use the mathematical model of two-fluid MHD in order to take into account some important linear and nonlinear effects in the low-frequency short-scale AWs. In two-fluid MHD the electron and ion fluids are allowed to move in separate ways, but are coupled by collective electromagnetic fields and by the electron-ion friction force. The equations of motion for the electrons and ions are:

$$\frac{\partial \mathbf{v}_e}{\partial t} + (\mathbf{v}_e \nabla)\, \mathbf{v}_e = -\frac{e}{m_e}\left(\mathbf{E} + \frac{1}{c}\mathbf{v}_e \times \mathbf{B}\right) - \frac{T_e}{m_e n_e}\nabla n_e + \mathbf{R}_{\|}, \tag{4}$$

$$\frac{\partial \mathbf{v}_i}{\partial t} + (\mathbf{v}_i \nabla)\, \mathbf{v}_i = \frac{e}{m_i}\left(\mathbf{E} + \frac{1}{c}\mathbf{v}_i \times \mathbf{B}\right) - \frac{T_i}{m_i n_i}\nabla n_i - \frac{m_e}{m_i}\mathbf{R}_{\|}, \tag{5}$$

where $p_{e,i} = n_{e,i} T_{e,i}$ is the ion/electron pressure, $T_{e,i} = const$ (but we do not require $T_e = T_i$). The parallel friction force, $\mathbf{R}_{\|} \,\|\mathbf{B}_0$, responsible for the (parallel) resistivity along $\mathbf{B}_0$, is

$$\mathbf{R}_{\|} = -\nu\left(\mathbf{v}_{e\|} - \mathbf{v}_{i\|}\right),$$

where $\nu = 0.51\nu_e$, ν_e is the electron collision frequency.

Note that we have dropped the perpendicular friction force, responsible for the perpendicular resistivity, because its contribution in the wave dissipation is $\left(\lambda_{\|}/\lambda_{\perp}\right)^2$ times smaller than contribution of the parallel resistivity ($\lambda_{\|}$ and $\lambda_{\perp}$ are the parallel and perpendicular wavelengths).

The particles number densities obey the continuity equations

$$\frac{\partial}{\partial t} n_s + \nabla(n_s \mathbf{v}_s) = 0, \tag{6}$$

where the subscript s denotes particles species, $s = e, i$.

3. Alfvén wave eigenmode equation

Instead of the number density n_s, it is convenient to introduce the Boltzman-like potentials

$$\phi_s = -\frac{T_s}{q_s}\ln\frac{n_s}{n_n}, \tag{7}$$

where $q_s = e$ for ions and $-e$ for electrons, and n_n is a constant (in a uniform plasma, one can take the equilibrium number density n_0 for n_n). Then, by separating background and perturbed magnetic field $\mathbf{B} \to \mathbf{B}_0 + \mathbf{B}$, we can rewrite the Eqs. (4)-(6) as

$$\frac{\partial \mathbf{v}_s}{\partial t} = \frac{q_s}{m_s}\left(\frac{1}{c}\mathbf{v}_s \times \mathbf{B}_0 + \mathfrak{E}_s\right), \tag{8}$$

$$\frac{\partial}{\partial t}\phi_s + \mathbf{v}_s \cdot \nabla\phi_s - \frac{m_s}{q_s} V_{T\alpha}^2 \nabla \cdot \mathbf{v}_s = 0. \tag{9}$$

The function $\mathfrak{E}_s$ is the charge force per unit mass and unit charge, which includes the linear electric force, the collisional friction force, the pressure gradient force, and the nonlinear force:

$$\mathfrak{E}_s = \mathbf{E} - \frac{\nu m_e}{n e^2}\mathbf{j}_{\|} + \nabla\phi_s + \mathbf{f}_s. \tag{10}$$

The velocity difference is expressed through the current (the quasineutrality condition $n_e = n_i \equiv n$ is used):

$$(\mathbf{v}_i - \mathbf{v}_e) = \frac{1}{ne}\mathbf{j}, \tag{11}$$

and the nonlinear force is

$$\mathbf{f}_s = \frac{1}{c}\mathbf{v}_s \times \mathbf{B} - \frac{m_s}{q_s}(\mathbf{v}_s \cdot \nabla)\, \mathbf{v}_s. \tag{12}$$

Note that the functions ϕ_s in (7)-(10) contain both linear and nonlinear parts.

Multiplying $\mathbf{B}_0 \times (8)$ we find

$$\frac{\partial}{\partial t}\mathbf{v}_s \times \mathbf{B}_0 = \frac{q_s}{m_s}\left[-\mathbf{B}_0 \times \mathfrak{E}_s - \frac{1}{c}\mathbf{B}_0^2 \mathbf{v}_s + \frac{1}{c}(\mathbf{B}_0 \cdot \mathbf{v}_s)\, \mathbf{B}_0\right]. \tag{13}$$

Inserting this into $\partial(8)/\partial t$, we get an equation for the velocity in the plane $\perp \mathbf{B}_0$ as

$$\left(1 + \frac{1}{\Omega_s^2}\frac{\partial^2}{\partial t^2}\right)\frac{\partial}{\partial t}\mathbf{v}_{s\perp} = \frac{q_s}{m_s}\frac{1}{\Omega_s}\frac{\partial}{\partial t}\left[\frac{1}{\Omega_s}\frac{\partial}{\partial t}\mathfrak{E}_{s\perp} - \mathbf{b}_0 \times \mathfrak{E}_{s\perp}\right], \tag{14}$$

where $\mathbf{b}_0 = \mathbf{B}_0/B_0$ is the unit vector in the direction of equilibrium magnetic field (that is $\mathbf{E}_{\|} = \mathbf{b}_0 E_{\|}$, etc.), Ω_s is the cyclotron frequency.

For the motions that are slower than the cyclotron gyration of the particles, as the low-frequency MHD waves, the electron and ion velocities in the plane, normal to $\mathbf{B}_0$, may be found in a drift approximation:

$$\frac{\partial}{\partial t}\mathbf{v}_{s\perp} = \frac{q_s}{m_s}\frac{1}{\Omega_s}\frac{\partial}{\partial t}\left[\frac{1}{\Omega_s}\frac{\partial}{\partial t}\mathfrak{E}_{s\perp} - \mathbf{b}_0 \times \mathfrak{E}_{s\perp}\right]. \tag{15}$$

The velocity of the particles along the magnetic field follows the equation

$$\frac{\partial}{\partial t}\mathbf{v}_{s\|} = \frac{q_s}{m_s}\mathfrak{E}_{s\|}. \tag{16}$$

Using (14) and (13), we eliminate the particle velocity from the continuity Eq. (9):

$$\frac{\partial^2}{\partial t^2}\phi_s + \frac{\partial}{\partial t}(\mathbf{v}_s \cdot \nabla\phi_s) - V_{T\alpha}^2 \nabla \cdot \left(\mathfrak{E}_{s\|} + \frac{1}{\Omega_s}\frac{\partial}{\partial t}\left[\frac{1}{\Omega_s}\frac{\partial}{\partial t}\mathfrak{E}_{s\perp} - \mathbf{b}_0 \times \mathfrak{E}_{s\perp}\right]\right) = 0, \tag{17}$$

or, inserting the explicit expression for $\mathfrak{E}_s$,

$$\frac{\partial^2}{\partial t^2}\left(1-V_{T\alpha}^2\nabla\cdot\frac{1}{\Omega_s^2}\nabla_\perp\right)\phi_s - V_{T\alpha}^2\nabla\cdot\nabla_\parallel\phi_s + V_{T\alpha}^2\nabla\cdot\frac{1}{\Omega_s}\frac{\partial}{\partial t}\left[\mathbf{b}_0\times\nabla_\perp\phi_s\right] = V_{T\alpha}^2\nabla\cdot\left(\left(\mathbf{E}-\frac{m_e\nu}{ne^2}\mathbf{j}\right)_\parallel + \frac{1}{\Omega_s^2}\frac{\partial^2}{\partial t^2}\mathbf{E}_\perp - \frac{1}{\Omega_s}\frac{\partial}{\partial t}\left[\mathbf{b}_0\times\mathbf{E}_\perp\right]\right) - \frac{\partial}{\partial t}\left(\mathbf{v}_s\cdot\nabla\phi_s\right) + V_{T\alpha}^2\nabla\cdot\left(\mathbf{f}_{s\parallel} + \frac{1}{\Omega_s^2}\frac{\partial^2}{\partial t^2}\mathbf{f}_{s\perp} - \frac{1}{\Omega_s}\frac{\partial}{\partial t}\left[\mathbf{b}_0\times\mathbf{f}_{s\perp}\right]\right); \quad (18)$$

here $V_{T\alpha}^2 = T_\alpha/m_\alpha$. Taking into account the quasineutrality condition, $-(T_e/T_i)\,\phi_i = \phi_e \equiv \phi$, and neglecting coupling to the fast magnetosonic waves (via terms with vector products), we rewrite the continuity Eq. (18) for electrons and ions separately:

$$V_{Te}^{-2}\left(\frac{\partial^2}{\partial t^2}\phi - V_{Te}^2\nabla\cdot\nabla_\parallel\phi\right) = \nabla\cdot\left(\mathbf{E}-\nu\frac{m_e}{ne^2}\mathbf{j}\right)_\parallel + N_e; \quad (19)$$

$$\frac{m_i}{m_e}V_{Te}^{-2}\left(\frac{\partial^2}{\partial t^2}\left(1-V_{Ti}^2\nabla\cdot\frac{1}{\Omega^2}\nabla_\perp\right)\phi - V_{Ti}^2\nabla\cdot\nabla_\parallel\phi\right) = -\nabla\cdot\left(\left(\mathbf{E}-\nu\frac{m_e}{ne^2}\mathbf{j}\right)_\parallel + \frac{1}{\Omega^2}\frac{\partial^2}{\partial t^2}\left(\mathbf{E}-\nu\frac{m_e}{ne^2}\mathbf{j}\right)_\perp\right) - N_i, \quad (20)$$

where N_e and N_i denote the following nonlinear terms:

$$N_e = -V_{Te}^{-2}\frac{\partial}{\partial t}\left(\mathbf{v}_e\cdot\nabla\phi_e\right) + \nabla\cdot\left(\mathbf{f}_{e\parallel} + \frac{1}{\Omega_e^2}\frac{\partial^2}{\partial t^2}\mathbf{f}_{e\perp} - \frac{1}{\Omega_e}\frac{\partial}{\partial t}\left[\mathbf{b}_0\times\mathbf{f}_{e\perp}\right]\right); \quad (21)$$

and

$$N_i = \frac{T_i}{T_e}V_{Ti}^{-2}\frac{\partial}{\partial t}\left(\mathbf{v}_i\cdot\nabla\phi\right) + \nabla\cdot\left(\mathbf{f}_{i\parallel} + \frac{1}{\Omega^2}\frac{\partial^2}{\partial t^2}\mathbf{f}_{i\perp} - \frac{1}{\Omega}\frac{\partial}{\partial t}\left[\mathbf{b}_0\times\mathbf{f}_{i\perp}\right]\right), \quad (22)$$

One more equation is obtained from the parallel component of Ampére's law:

$$\frac{\partial}{\partial t}\frac{c}{4\pi en}\left[\nabla\times\mathbf{B}\right]_\parallel = \frac{\partial}{\partial t}\frac{1}{en}j_\parallel = \left(\frac{\partial}{\partial t}v_{i\parallel} - \frac{\partial}{\partial t}v_{e\parallel}\right) = \frac{e}{m_e}\left(\frac{m_e}{m_i}\mathfrak{E}_{i\parallel} + \mathfrak{E}_{e\parallel}\right), \quad (23)$$

or, explicitly,

$$\nabla_\parallel\phi = -\left(\mathbf{E}-\nu\frac{m_e}{ne^2}\mathbf{j}\right)_\parallel - \delta_e^2\left[\nabla\times\nabla\times\mathbf{E}\right]_\parallel + N_{ei}, \quad (24)$$

where the electron skin length $\delta_e^2 = c^2/\omega_{pe}^2$ and the nonlinear term

$$N_{ei} = -\delta_e^2\frac{e}{cT_e}\left[\nabla\times\mathbf{B}\right]_\parallel\frac{\partial}{\partial t}\phi - \left[\frac{m_e}{m_i}\mathbf{f}_{i\parallel} + \mathbf{f}_{e\parallel} + \frac{n}{n_0}\left(\mathbf{E}-\frac{\nu}{ne^2}\mathbf{j}+\nabla\phi\right)_\parallel\right], \quad (25)$$

The set of Eqs. (19), (20) and (22) constitute a basis for the investigation of linear and nonlinear properties of short-scale Alfvén waves. Further simplification may be achieved by expressing the electromagnetic fields through electromagnetic potentials. A usual choice is φ and $\mathbf{A}$, such that

$$\mathbf{E} = -\nabla\varphi - \frac{1}{c}\frac{\partial}{\partial t}\mathbf{A}$$

and

$$\mathbf{B} = \nabla\times\mathbf{A}.$$

However, here it is convenient to introduce an effective potential ψ for the field-aligned inductive (solenoidal) part of electric field,

$$\mathbf{E}_{A\parallel} = -\nabla_\parallel\psi,$$

so that ψ is related to the parallel component of the potential $\mathbf{A}$ through the equation

$$-\frac{1}{c}\frac{\partial}{\partial t}A_\parallel = -\nabla_\parallel\psi.$$

The potential part of the electric field is described by the usual potential φ:

$$\mathbf{E}_\varphi = -\nabla\varphi.$$

This choice enables us to express both φ and ϕ in terms of ψ. Namely, insertion $\nabla_\parallel\phi$ from (22) into (19) gives ϕ in terms of ψ (note that only the inductive part of the electric field enters Ampére's law):

$$V_{Te}^{-2}\frac{\partial^2}{\partial t^2}\phi = -\nabla_\parallel^2\delta_e^2\nabla^2\psi + \nabla_\parallel\cdot N_{ei} + N_e. \quad (26)$$

Furthermore, when we apply the inverse operator $\nabla_\parallel^{-2}$ to (19) we get a formal solution with respect to φ:

$$\varphi = -\psi + \phi - V_{Te}^{-2}\nabla_\parallel^{-2}\frac{\partial^2}{\partial t^2}\phi - \nabla_\parallel^{-\mathbf{2}}\nabla\cdot\nu\frac{m_e}{ne^2}\mathbf{j}_\parallel + \nabla_\parallel^{-2}N_e. \quad (27)$$

Inserting this into (20) we get

$$-\frac{m_i}{m_e}V_{Te}^{-2}\left[\frac{\partial^2}{\partial t^2}\left(1-V_T^2\nabla\cdot\frac{1}{\Omega^2}\nabla_\perp\right) - V_T^2\nabla\cdot\nabla_\parallel + \frac{m_e}{m_i}\frac{\partial^2}{\partial t^2} + \frac{m_e}{m_i}\frac{1}{\Omega^2}\frac{\partial^2}{\partial t^2}\nabla_\perp^2\nabla_\parallel^{-2}\frac{\partial^2}{\partial t^2}\right]\phi = N_i - N_e - \frac{1}{\Omega^2}\frac{\partial^2}{\partial t^2}\nabla_\perp^2\left[-\psi - \nabla_\parallel^{-\mathbf{2}}\nabla\cdot\nu\frac{m_e}{ne^2}\mathbf{j}_\parallel + \nabla_\parallel^{-2}N_e\right] + \nabla_\perp\frac{1}{\Omega^2}\frac{\partial^2}{\partial t^2}\mathbf{E}_{A\perp}, \quad (28)$$

where $V_T^2 = (1+T_e/T_i)V_{Ti}^2$. We can now remove ϕ from Eq. (28) by means of (26):

$$\frac{m_i}{m_e}\left[\frac{\partial^2}{\partial t^2}\left(1+\frac{m_e}{m_i} - V_T^2\nabla\cdot\frac{1}{\Omega^2}\nabla_\perp\right) - V_T^2\nabla\cdot\nabla_\parallel + \frac{m_e}{m_i}\frac{1}{\Omega^2}\frac{\partial^2}{\partial t^2}\nabla_\perp^2\nabla_\parallel^{-2}\frac{\partial^2}{\partial t^2}\right]\nabla_\parallel^2\delta_e^2\nabla^2\psi - \frac{1}{\Omega^2}\frac{\partial^2}{\partial t^2}\frac{\partial^2}{\partial t^2}\nabla^2\psi =$$

$$\frac{m_i}{m_e}\left[\frac{\partial^2}{\partial t^2}\left(1+\frac{m_e}{m_i}-V_T^2\nabla\cdot\frac{1}{\Omega^2}\nabla_\perp\right)-V_T^2\nabla\cdot\nabla_\parallel+\right.$$
$$\left.\frac{m_e}{m_i}\frac{1}{\Omega^2}\frac{\partial^2}{\partial t^2}\nabla_\perp^2\nabla_\parallel^{-2}\frac{\partial^2}{\partial t^2}\right]\left(\nabla_\parallel\cdot N_{ei}+N_e\right)+$$
$$\frac{\partial^2}{\partial t^2}\left[N_i-N_e\right]-$$
$$\frac{1}{\Omega^2}\frac{\partial^2}{\partial t^2}\nabla^2\frac{\partial^2}{\partial t^2}\left(\nabla_\parallel^{-\mathbf{2}}\nabla\cdot\nu\frac{m_e}{ne^2}\mathbf{j}_\parallel+\nabla_\parallel^{-2}N_e\right). \quad (29)$$

When we multiply this equation by $\Omega^2\nabla_\parallel^2\delta_e^2$ and treating the right-hand part as a perturbation, we get the eigenmode equation

$$\left\{\nabla_\parallel^2V_A^2\left[\frac{\partial^2}{\partial t^2}\left(1+\frac{m_e}{m_i}-V_T^2\nabla\cdot\frac{1}{\Omega^2}\nabla_\perp\right)-V_T^2\nabla_\parallel^2\right]\right.$$
$$\left.-\frac{\partial^4}{\partial t^4}\left(1-\delta_e^2\nabla_\perp^2\right)-\nu\frac{\partial}{\partial t}\frac{\partial^2}{\partial t^2}\delta_e^2\nabla^2\right\}\nabla_\parallel^2\delta_e^2\nabla^2\psi=$$
$$\frac{\partial^2}{\partial t^2}\left\{\frac{\partial^2}{\partial t^2}\left(\nabla_\parallel N_{ei}+N_e\right)+\right.$$
$$\left.\frac{m_e}{m_i}\left[\nabla_\parallel^2V_A^2\left(N_i-N_e\right)-\delta_i^2\nabla^2\frac{\partial^2}{\partial t^2}N_e\right]\right\}. \quad (30)$$

where the collisional term is expressed in terms of ψ,

$$\frac{\partial}{\partial t}\nabla\cdot\frac{m_e}{ne^2}j_\parallel=\nabla\cdot\frac{c^2m_e}{4\pi ne^2}\left[\nabla\times\frac{1}{c}\frac{\partial}{\partial t}\mathbf{B}\right]_\parallel=\nabla_\parallel^2\delta_e^2\nabla^2\psi.$$

The differential order of this equation may be reduced by dropping the term $\sim V_T^2\nabla_\parallel^2$, which has a small effect on the Alfvén wave branch in a low-β plasma:

$$\left\{V_A^2\nabla_\parallel^2\left(1-V_T^2\nabla\cdot\frac{1}{\Omega^2}\nabla_\perp\right)-\frac{\partial^2}{\partial t^2}\left(1-\delta_e^2\nabla_\perp^2\right)-\right.$$
$$\left.\nu\frac{\partial}{\partial t}\delta_e^2\nabla^2\right\}\nabla_\parallel^2\delta_e^2\nabla^2\psi=\frac{\partial^2}{\partial t^2}\left(\nabla_\parallel N_{ei}+N_e\right)+$$
$$\frac{m_e}{m_i}\left[\nabla_\parallel^2V_A^2\left(N_i-N_e\right)-\delta_i^2\nabla^2\frac{\partial^2}{\partial t^2}N_e\right]. \quad (31)$$

In the above expressions $\bar\rho_i^2{=}V_T^2/\Omega_i^2=(1+T_e/T_i)V_{Ti}^2/\Omega_i^2$ and the ion skin-length $\delta_i^2=(m_i/m_e)\delta_e^2$.

Eq. (31) is the key equation of the present paper. It is the (second-order in $\partial/\partial t$) nonlinear Alfvén wave eigenmode equation in a non-uniform plasma. It contains the nonzero ion-gyroradius correction ($\sim V_T^2\nabla\cdot\Omega^{-2}\nabla_\perp$), the electron inertia correction ($\sim\delta_e^2\nabla_\perp^2$), and the collisional dissipative term ($\sim\nu$) in the linear (left-hand side) part. The nonlinear (right-hand side) part contains second-order terms coming from the electron and ion continuity equations ($\sim N_e$, N_i) and from the parallel component of Ampére's law ($\sim N_{ei}$).

The Alfvén mode Eq. (31) is linearly decoupled from the fast (slow) mode equation because the fast (slow) wave has much higher (lower) frequencies than the Alfvén wave for the same wavenumber and for large propagation angles. The nonlinear part of (31) contains the beatings of the pump AW with the fluctuations corresponding to different modes, including fast, Alfvén and slow modes. However, the secondary waves are effectively enhanced from the background noise by the beatings which are in resonance with the excited waves. Due to the separation of the oblique Alfvén mode from the other modes in the $(\omega-k)$ space, the resonance can occur with the low-wavenumber fast wave or with the low-frequency slow wave. These resonances are less efficient than the resonance among oblique Alfvén waves, which are close in the $(\omega-k)$ space. There are two other important properties of the fast and slow waves which make it difficult for them to be excited by the three-wave resonant interaction with Alfvén waves in the solar corona. The growth of the fast wave is suppressed by: (1) strong refraction of the isotropic ($\omega=\sqrt{k_z^2+k_\perp^2}V_A$) fast wave in a nonuniform plasma, quickly bringing the wave out of the resonance; (2) by ion temperature anisotropy $T_{i\perp}/T_{i\parallel}>1$, very probable in the corona in view of recent SOHO observations. The growth of the slow wave is suppressed by its strong Landau damping unless $T_e/T_i\gg1$, which is unlikely to be the case in the corona. Thereto, direct comparison shows that the increment (56) is much larger than the increment of decay into slow and fast waves (Yukhimuk et al. 1999).

On the contrary, the Alfvén mode is less sensitive to the above mentioned stabilizing factors and has a highly anisotropic dispersion making it possible for the wave triads to remain in resonance even in a nonuniform plasma. That is why our focus is on the excitation of highly oblique Alfvén waves by a highly oblique pump Alfvén wave set up by phase mixing due to plasma nonuniformity. The situation can be different with the parallel-propagating pump AW.

4. Alfvén wave phase mixing and collisional dissipation in corona

Consider the evolution of an AW, excited at the magnetic field lines, where the length scale of the transverse inhomogeneity of the equilibrium is $L_\perp$ and the length scale of the field-aligned inhomogeneity of the equilibrium is $L_\parallel$. Both $L_\perp$ and $L_\parallel$ can vary over a wide range in the solar corona, but usually $L_\parallel\gg L_\perp$. Take a wave frequency for which the parallel wavelength $\lambda_\parallel$ is much shorter than the length-scale of the field-aligned equilibrium inhomogeneity, $\lambda_\parallel<L_\parallel$. Then, as the wave propagates, the perpendicular length-scale of the wave decreases in time as $\lambda_\perp/L_\perp=\tau_A/t$ (τ_A is the wave period). Therefore, even if the initially excited AW has a smooth distribution in the direction of the plasma inhomogeneity, phase mixing creates short wave length-scales $\lambda_\perp<L_\perp$ in a few wave periods. In open magnetic configurations, where waves propagate upward from the footpoints, this corresponds to heights of the order of a few field-aligned wavelengths. From now on we shall study the dynamics of Alfvén waves, in which short perpendicular wavelengths, $\lambda_\perp<L_\perp$, are either initially determined by a (unspecified) generator, or are created by phase-mixing.

In this situation we consider the evolution of the ω-th harmonic of the wave field using a WKB-ansatz:

$$A=A_0\times\exp\left(-i\omega t+i\int\mathbf{k}\cdot\mathbf{dr}+\int\gamma dt\right). \quad (32)$$

The wave vector $\mathbf{k}$ and the growth/damping rate γ have to be calculated from the local dispersion relation, and the integration

is along the path of the wave propagation. The effects of plasma inhomogeneity for these waves come about through the spatial dependence of the plasma parameters along the path of the wave propagation. This path is determined by the ray equations for the wave vector $\mathbf{k}$ and position $\mathbf{r}$:

$$\frac{d\mathbf{k}}{dt} = -\frac{\partial\omega}{\partial\mathbf{r}} = -\omega\left(\frac{1}{V_A}\frac{\partial V_A}{\partial\mathbf{r}}\right); \tag{33}$$

$$\frac{d\mathbf{r}}{dt} = \frac{\partial\omega}{\partial\mathbf{k}}. \tag{34}$$

In accordance with the above, the wave frequency here is determined by the local dispersion relation found from the dynamic Eq. (31) for Alfvén waves. When we neglect the nonlinear terms in (30), we get the linear Alfvén wave frequency, ω, and the linear damping rate, γ_c, which accounts for the thermal and electron inertia effects, and for electron-ion collisions:

$$\omega^2 = k_\parallel^2 V_A^2\left[\frac{1+k_\perp^2\bar{\rho}_i^2}{1+k_\perp^2\delta_e^2} - \beta\frac{1}{1+k_\perp^2\bar{\rho}_i^2}\right]; \tag{35}$$

$$\gamma_c = -0.5\nu\frac{k_\perp^2\delta_e^2}{1+k_\perp^2\delta_e^2}\left[1+\beta\frac{\left(1+k_\perp^2\delta_e^2\right)^5}{\left(1+k_\perp^2\bar{\rho}_i^2\right)^2}\right], \tag{36}$$

where $\beta = V_T^2/V_A^2$. Since we ignore the magnetic compressibility, $\beta < 1$. For a low-β plasma, a good approximation to (35) and (36) in a wide range of parameters is

$$\omega^2 = k_\parallel^2 V_A^2\frac{1+k_\perp^2\bar{\rho}_i^2}{1+k_\perp^2\delta_e^2}; \tag{37}$$

$$\gamma_c = -0.5\nu\frac{k_\perp^2\delta_e^2}{1+k_\perp^2\delta_e^2}. \tag{38}$$

When we neglect the electron inertia term, we find the AW dispersion to be close to the KAW dispersion, known from the kinetic theory (Hasegawa & Chen 1976), for all values of the dispersion parameter $k_\perp^2\bar{\rho}_i^2$. In the limit $k_\perp^2\bar{\rho}_i^2 \gg 1$ they are identical.

It is convenient to introduce the dispersion function $K(k_\perp)$:

$$K^2(k_\perp) = \frac{1+k_\perp^2\bar{\rho}_i^2}{1+k_\perp^2\delta_e^2}, \tag{39}$$

and to write the AW dispersion relation in the form

$$\omega = k_z V_A K(k_\perp).$$

The function $K(k_\perp)$ is the factor by which the parallel phase velocity of the AWs with perpendicular wavelength $2\pi/k_\perp$ exceeds V_A.

In the case of weak AW dispersion ($k_\perp^2\delta_e^2,\ k_\perp^2\bar{\rho}_i^2 \ll 1$), $K(k_\perp) \simeq 1$, we recover by means of Eq. (36) the asymptotic result of Heyvaerts & Priest (1983) for the wave damping with height z:

$$A = A_0\times\exp\left(\int\gamma_c\left(\frac{\partial\omega}{\partial k_z}\right)^{-1}dz\right) = A_0\times\exp\left(-\frac{z^3}{z_c^3}\right), \tag{40}$$

where z_c is the characteristic height of the resistive (collisional) wave dissipation,

$$z_c = \left[\frac{1}{12}\frac{m_e}{m_i}\frac{\nu_e}{V_A L_A^2}\right]^{-\frac{1}{3}}\left(\frac{\omega}{\Omega_i}\right)^{-\frac{2}{3}}. \tag{41}$$

However, in addition to collisional dissipation, the small-scale AWs undergo also nonlinear interaction, described by the right-hand side of (31). Therefore, the amplitude of the pump AW changes not only because of collisional dissipation, but also due to nonlinear interaction. Nonlinear AWs interaction and the question which process dominates for given plasma and wave parameters is investigated in the following sections.

5. Parametric decay and damping of the phase-mixed AW in the corona

5.1. Dynamic equation and coupling coefficients of the three-wave AW interaction

We shall proceed further in the local approximation and expand all perturbations that appear in the eigenmode Eq. (31) into Fourier series. We use the second-order approximation for all quantities, which are present in the nonlinear right-hand side, expressing all perturbations through the parallel component of the electromagnetic potential A_z. Then, we average over time and space intervals which are short compared to the intervals over which the amplitudes of the waves vary, but $\omega\triangle t \ll 1$, $\mathbf{k}\cdot\triangle\mathbf{r} \ll 1$, and obtain the dynamic equations describing the slow variations of the wave amplitude:

$$\left(\frac{\partial}{\partial t} + \mathbf{v}_k\cdot\nabla - \gamma_k\right)A_k^\sigma = \sum_{1,2}\delta(\sigma\mathbf{k}-\sigma_1\mathbf{k_1}-\sigma_2\mathbf{k_2})\delta\left(\sigma\omega_k - \sigma_1\omega_1 - \sigma_2\omega_2\right) U_{s_1,s_2}(\sigma\mathbf{k},\sigma_1\mathbf{k}_1,\sigma_2\mathbf{k}_2)A_1^{\sigma_1}A_2^{\sigma_2}, \tag{42}$$

where $s_i = \mp 1$ for $k_{iz} \lessgtr 0$, $i = k, 1, 2$ (k_z is chosen to be > 0).

The coefficients $s_{1,2} = \pm 1$ in the Eq. (42) take into account that the phase velocity of μ-th wave, $V_\mu = \omega_\mu/k_{\mu z}$, can be positive ($V_\mu > 0$ with $k_{\mu z} > 0$) or negative ($V_\mu < 0$ with $k_{\mu z} < 0$), and the indices σ, σ_1 and σ_2 denote complex conjugate terms $A_\mu^{+1} \equiv A_\mu$ and $A_\mu^{-1} \equiv A_\mu^*$ (note that only real parts, $\mathrm{Re}A_\mu = 0.5\left(A_\mu + A_\mu^*\right)$, should be taken of the complex amplitudes in binary combinations).

The coupling coefficient of the three-wave resonant interaction is

$$U_{s,s_1,s_2}(\sigma\mathbf{k},\sigma_1\mathbf{k}_1,\sigma_2\mathbf{k}_2) = \frac{V_A}{4B_0}(s_1K_1 - s_2K_2)\frac{K_k}{\varkappa^2}\left(s_1\frac{\varkappa_1^2}{K_1} + s_2\frac{\varkappa_2^2}{K_2} + s\frac{\varkappa^2}{K_k}\right)\sigma_1\sigma_2\left(\mathbf{k}_1\times\mathbf{k}_2\right)_z, \tag{43}$$

where $\varkappa = k_\perp\bar{\rho}_i$ is the kinetic factor, accounting for temperature (FLR and electron pressure) effects. From (43) we see that three-wave resonant interaction among AWs is local in k-space, i.e. the wavenumbers of the effectively interacting AWs are of the same order, $k_\perp \sim k_{1\perp} \sim k_{2\perp}$. Note that the non-zero

value of $U(\mathbf{k},\mathbf{k}_1,\mathbf{k}_2)$ and the non-linear (three-wave) coupling among AW triads becomes possible due to the finite value of the kinetic factor $\varkappa$. In MHD Alfvén waves $\varkappa_\mu = 0$, making $K = K_1 = K_2 = 1$ so that $U(\mathbf{k},\mathbf{k}_1,\mathbf{k}_2) = 0$ for resonant triads in agreement with the well-known fact that three-wave resonant interaction is impossible among ideal MHD Alfvén waves.

Since we consider AWs with frequencies $\omega^2 \ll \Omega^2$ in a low-β coronal plasma, we have dropped the terms of the order $\sim \omega^2/\Omega^2$ and $\sim \beta$ in comparison to those retained in the expression for the matrix element (43). In this situation, the most important effect for parametric decay is the vector nonlinearity, $\sim (\mathbf{k}_1 \times \mathbf{k}_2)_z$, retained in (43). The converse situation, where the scalar nonlinearity, $\sim \mathbf{k}_1 \cdot \mathbf{k}_2$, becomes more important, is considered by Voitenko & Goossens (in preparation).

The matrix element $U(\mathbf{k},\mathbf{k}_1,\mathbf{k}_2)$ is the key mathematical object in the non-linear wave theory. Once this matrix element is found, we can follow theoretical methods developed earlier in order to study nonlinear properties of a given mode.

Using expressions (42)-(43), we study the parametric decay of AWs in the next section. This nonlinear process is important for the AWs and often plays a crucial role in wave propagation, nonlinear saturation of instabilities, and spectral dynamics (Voitenko 1998a,b).

5.2. Parametric decay instability of the short-scale Alfvén waves

The parametric decay of a pump oblique AW into two daughter oblique AWs in a hot plasma has been first examined by Erokhin et al. (1978), followed by other authors (see e.g. Volokitin & Dubinin 1989; Voitenko 1996c; Yukhimuk & Kucherenko 1993). The common approach so far was to consider weak wave dispersion, $k_\perp^2 \bar{\rho}_i^2 \ll 1$, and to assume that all three interacting AWs propagate in the same direction along the background magnetic field. However, it was shown in the framework of kinetic theory by Voitenko (1998a) that the strongest decay of the weakly dispersing AW was missed in the previous investigations. Indeed, the strongest decay occurs when the daughter waves propagate in opposite directions along the background magnetic field. Also, in contrast with previous studies, we consider the influence of resistive dissipation of AWs and the detuning of the perpendicular wavenumbers, caused by the transverse inhomogeneity. The inclusion of these effects is important when investigating the phase mixing of the low-frequency part of the AWs in the corona. Hence, we shall study the KAW decay instability for an arbitrary value of the kinetic factor $\varkappa$, based on the dynamic Eq. (42) found from the two-fluid resistive MHD plasma model.

Let us consider a pump KAW with frequency ω_k, wave vector $\mathbf{k}$, and amplitude A_k, propagating in the positive z-direction, i.e. $k_z > 0$. From (42) it follows that the waves $(\omega_1,\mathbf{k}_1,A_1)$ and $(\omega_2,\mathbf{k}_2,A_2)$ can effectively interact with the pump wave, provided the following resonant conditions:

$$\mathbf{k}_1 + \mathbf{k}_2 \;=\; \mathbf{k};$$

$$\omega_1 + \omega_2 \;=\; \omega_k \tag{44}$$

are satisfied. The dynamical equations for waves **1** and **2**, coupled via the parametric pump wave, are:

$$\left(\frac{\partial}{\partial t} - \gamma_1\right) A_1 = -U(\mathbf{k}_1,\mathbf{k},-\mathbf{k}_2) A_k A_2^*; \tag{45}$$

$$\left(\frac{\partial}{\partial t} - \gamma_2\right) A_2^* = -U(-\mathbf{k}_2,-\mathbf{k},\mathbf{k}_1) A_k^* A_1. \tag{46}$$

Acting by the operator $(\partial/\partial t - \gamma_2)$ on the Eq. (45) and eliminating A_2^* by use of Eq. (46), we obtain the equation for the amplitude A_1 (the corresponding equation for the amplitude A_2 is obtained in the same way):

$$\left(\frac{\partial^2}{\partial t^2} - (\gamma_1+\gamma_2)\frac{\partial}{\partial t} + \gamma_1\gamma_2\right) A_{1,2} = U(\mathbf{k}_1,\mathbf{k},-\mathbf{k}_2) U(-\mathbf{k}_2,-\mathbf{k},\mathbf{k}_1) \left|A_k\right|^2 A_{1,2}. \tag{47}$$

An exponential solution to (47), $\sim \exp(\delta t)$, has indices

$$\delta = \frac{\gamma_1+\gamma_2}{2} \pm \sqrt{\left(\frac{\gamma_1-\gamma_2}{2}\right)^2 + \gamma_{NL}^2},$$

where the rate of non-linear interaction is

$$\gamma_{NL}^2 \;=\; \Omega_i^2 \left(\frac{V_A}{4V_{Ti}}\right)^2 \frac{K_1 K_2 (K_2 - s_2 K_k)(s_1 K_k - K_1)}{\varkappa^2 \varkappa_1^2 \varkappa_2^2} \left(s_1 \frac{\varkappa_1^2}{K_1} + s_2 \frac{\varkappa_2^2}{K_2} + \frac{\varkappa^2}{K_k}\right)^2 \left|\varkappa_1 \times \varkappa_2\right|_z^2 \left|\frac{B_k}{B_0}\right|^2. \tag{48}$$

The waves 1 and 2 grow if

$$\delta > 0. \tag{49}$$

For the rate of the non-linear interaction γ_{NL} to be real, i.e. $\gamma_{NL}^2 > 0$, the dispersion functions K_μ have to satisfy the decay condition that

$$(K_2 - s_2 K_k)(s_1 K_k - K_1) > 0. \tag{50}$$

In the case of weak wave-particles interaction, $\gamma_1, \gamma_2 \ll \gamma_{NL}$, the growth rate of the waves 1 and 2 is determined by the rate of the non-linear interaction: $\delta \sim \gamma_{NL}$.

The decay condition (50) implies that at least one dispersion function of the decay product should be smaller than the dispersion function of the pump wave ($\gamma_{NL}^2 < 0$ for arbitrary s_1 and s_2 if both K_1 and $K_2 > K_k$). In what follows we choose $K_1 < K_k$, so that decay is possible: into (1) parallel-propagating daughter KAWs, $k_{1z} > 0$, $k_{2z} > 0$ ($s_1 = s_2 = 1$), and into (2) counterstreaming daughter KAWs, $k_{1z} > 0$, $k_{2z} < 0$ ($s_1 = 1$, $s_2 = -1$) (here $k_z > 0$ is chosen for the pump wave).These decay channels are shown on Fig. 1 as parallelograms in the (ω, k_z)-plane, reflecting matching conditions for corresponding AW triads.

Let us consider these two cases separately for the weakly dispersed KAWs, $\varkappa^2, \varkappa_1^2, \varkappa_2^2 \ll 1$ (we shall not consider here strongly dispersed AWs, $\varkappa^2, \varkappa_1^2, \varkappa_2^2 \gg 1$, which are unlikely for the AW phase-mixing in corona).

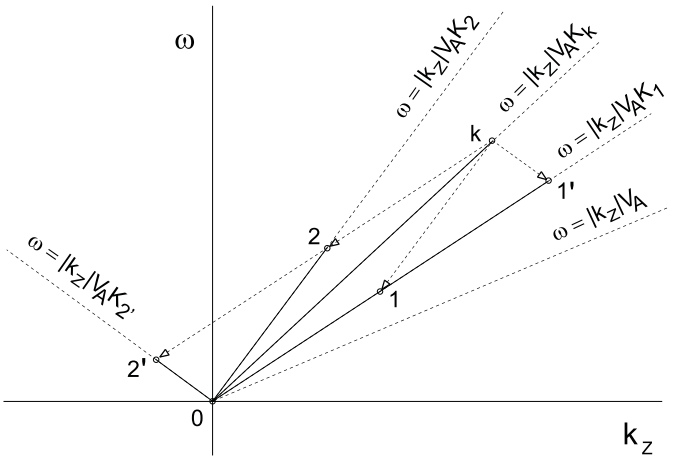

Fig. 1. Two possible channels for decay of the pump KAW k: 1) decay into two parallel-propagating KAWs $k \to 1+2$ ($k_{1z} > 0, k_{2z} > 0$); 2) decay into two counterstreaming KAWs $k \to 1' + 2'$ ($k'_{1z} > 0, k'_{2z} < 0$), where we have taken $k'_{1\perp} = k_{1\perp}$ for simplicity. The dispersion of the MHD Alfvén wave $\omega = |k_z|\, V_A$ is shown for reference.

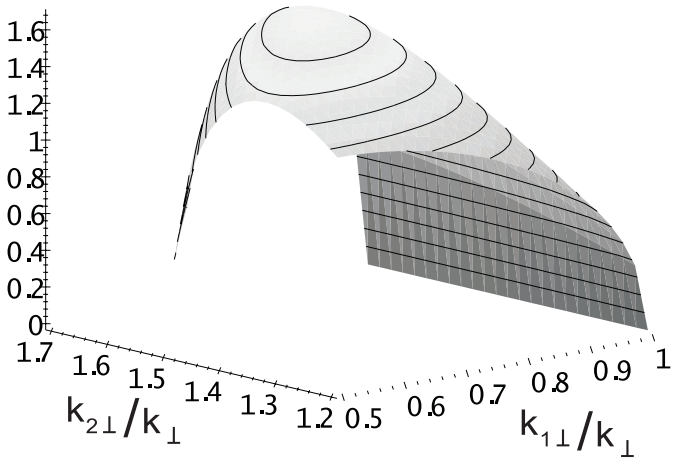

Fig. 2. The dependence of the normalized rate of parametric decay on the wavenumbers of the parallel-propagating decay waves, $k_{1\perp}/k_\perp$ and $k_{2\perp}/k_\perp$.

5.3. Excitation of the parallel-propagating decay AWs ($k_{1z} > 0$, $k_{2z} > 0$)

As follows from (50) with $s_1 > 0$ and $s_2 > 0$, the decay process including parallel-propagating KAWs $(\omega_k, \mathbf{k}, A_k) \to (\omega_1, \mathbf{k}_1, A_1) + (\omega_2, \mathbf{k}_2, A_2)$ can take place if the dispersion functions of the decay products K_1 and K_2 are smaller and larger respectively than the dispersion function K_k of the pump KAW:

$$K_1 < K_k < K_2. \tag{51}$$

Since the function K is a monotonous function of its argument $\varkappa$, we conclude that the wavenumbers of the interacting waves have to satisfy the following sequence of inequalities:

$$0 < k_{1\perp} < k_\perp < k_{2\perp} < 2k_\perp. \tag{52}$$

The last inequality here follows from a combination of the resonant condition for the wave vectors and the second inequality.

For $\varkappa^2, \varkappa_1^2, \varkappa_2^2 \ll 1$, we use the asymptotic expression $K\left(k_{\mu\perp}\right) = 1 + 0.5 k_{\mu\perp}^2 \bar{\rho}_i^2$ in (48) so that

$$\gamma_{NL} = \Omega_i \frac{V_A}{8V_{Ti}} \left(1 + \frac{T_e}{T_i}\right) \frac{(\varkappa^2 + \varkappa_1^2 + \varkappa_2^2)\sqrt{(\varkappa_2^2 - \varkappa_k^2)(\varkappa_k^2 - \varkappa_1^2)}}{\varkappa\varkappa_1\varkappa_2} |\varkappa_1 \times \varkappa_2|_z \left|\frac{B_k}{B_0}\right|. \tag{53}$$

The dependence of the normalized decay rate,

$$\bar{\gamma}_{NL} = \gamma_{NL} \left[\Omega_i \frac{V_A}{8V_{Ti}} \left(1 + \frac{T_e}{T_i}\right) \left|\frac{B_k}{B_0}\right| \varkappa^2\right]^{-1}, \tag{54}$$

on the wavenumbers of the decay waves is shown on the Fig. 2.

The spectrum of the generated daughter waves has a sharp maximum. To find the wavenumbers of the daughter waves which are most effectively excited, we determine the maximum of γ_{NL} given by (53) with respect to the wavenumbers of the decay products. Thus we obtain the rate of resonant decay instability into parallel-propagating AWs as

$$\gamma_{NL} = 0.4\Omega_i \frac{V_A}{V_{Ti}} \varkappa^3 \left|\frac{B_k}{B_0}\right|, \tag{55}$$

which is achieved for $\varkappa_1 = 0.717\varkappa$, $\varkappa_2 = 1.49\varkappa$ (here we take $T_e = T_i$ for simplicity).

Expression (55) shows a strong dependence of the interaction rate on the perpendicular wavenumber of the pump wave, $\gamma_{NL} \sim k_\perp^3$, and this results in a rapid decrease of the interaction rate with decreasing $k_\perp$.

5.4. Counterstreaming decay KAWs ($k_{1z} > 0$, $k_{2z} < 0$)

Eq. (53) is now replaced with

$$\gamma_{NL} = \Omega_i \frac{V_A}{4V_{Ti}} \sqrt{1 + \frac{T_e}{T_i}} \frac{(\varkappa^2 + \varkappa_1^2 - \varkappa_2^2)\sqrt{(\varkappa^2 - \varkappa_1^2)}}{\varkappa\varkappa_1\varkappa_2} |\varkappa_1 \times \varkappa_2|_z \left|\frac{B_k}{B_0}\right|. \tag{56}$$

The dependence of the normalized decay rate $\bar{\gamma}_{NL}$ on the wavenumbers,

$$\bar{\gamma}_{NL} = \gamma_{NL} \left(\Omega_i \frac{V_A}{4V_{Ti}} \sqrt{1 + \frac{T_e}{T_i}} \varkappa^2 \left|\frac{B_k}{B_0}\right|\right)^{-1} = \frac{(\varkappa^2 + \varkappa_1^2 - \varkappa_2^2)\sqrt{(\varkappa^2 - \varkappa_1^2)}}{\varkappa^3\varkappa_1\varkappa_2},$$

is shown on the Fig. 3.

When we compare the counterstreaming decay waves with the parallel-propagating decay AWs, we find that the spectrum of the counterstreaming decay waves is concentrated around another pair of wavenumbers: $\varkappa_1 = 0.776\varkappa$, $\varkappa_2 = 0.442\varkappa$. With these wavenumbers the maximum growth rate is

$$\gamma_k^{NL} = 0.3\Omega_i \frac{V_A}{V_{Ti}} \varkappa^2 \left|\frac{B_k}{B_0}\right|. \tag{57}$$

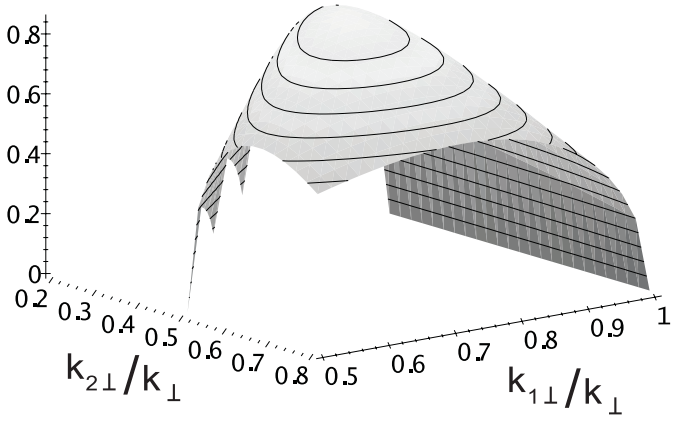

Fig. 3. The normalised rate of parametric decay depending on the wavenumbers of counterstreaming decay waves, $k_{1\perp}/k_\perp$ and $k_{2\perp}/k_\perp$.

With decreasing $k_\perp$, the decrease of the rate of decay into counterstreaming decay waves is not as strong as for parallel-propagating decay waves. This means that the decay into counterstreaming AWs is more effective for the weakly dispersing waves, created by phase mixing. Consequently, (57) gives a good approximation for the damping rate of the pump AW, and for the rate of the three-wave AWs interaction in **k**-space as well, if the decay into counterstreaming waves is not forbidden.

Summarizing, there are significant differences between the decay into parallel-propagating waves, and decay into counterstreaming (antiparallel-propagating) waves. Namely, the decay of a weakly-dispersing AW into counter-streaming waves:

1. is much stronger for a weakly dispersed AW in a homogeneous plasma, but
2. is more sensitive to the field-aligned inhomogeneity;
3. transfers the wave energy into lower wavenumbers only, $k_{s\perp} < k_{0\perp}$, thus reducing collisional dissipation, whereas the decay into parallel-propagating waves excite both shorter- and longer-wavelength waves, $k_{s\perp} \gtrless k_{0\perp}$;
4. in part, reverses the direction of wave energy propagation.

Expressions (55) and (57) will be used to estimate the nonlinear damping of the phase-mixed AWs with height in solar corona.

5.5. Collisional threshold of decay instability

Let us estimate the threshold amplitude for the decay instability of the phase-mixed pump in the corona, where the growth of the decay products due to nonlinear coupling via the pump wave may be balanced by their collisional dissipation. In a local approximation, the threshold amplitude for the pump wave to excite waves 1 and 2 is obtained from the marginal condition for decay (49), $\gamma_1\gamma_2 = \gamma_{NL}^2$, where γ_1 and γ_2 are to be determined from (38).

In the coronal plasma, the collisional damping is

$$\gamma_{cL(1,2)} \approx -0.5\nu k_{(1,2)\perp}^2 \delta_e^2, \tag{58}$$

and the marginal decay condition is

$$\gamma_{NL}^2 = 0.25\nu^2 k_{1\perp}^2 k_{2\perp}^2 \delta_e^4. \tag{59}$$

For the strongest counterstreaming decay (57), the threshold appears to be independent of the perpendicular wavenumbers or other wave characteristics, and the threshold value depends only on plasma parameters:

$$\left|\frac{B_k}{B_0}\right| = 0.57\frac{m_e}{m_i}\frac{\nu}{\Omega_i}\frac{V_A}{V_{Ti}}. \tag{60}$$

The actual value of the threshold with the typical coronal parameters is extremely low:

$$\left|\frac{B_k}{B_0}\right| = 10^{-6} - 10^{-7}. \tag{61}$$

The decay condition (49) is certainly satisfied for the AWs with $B_k/B_0 \sim 0.01$, able to heat the corona.

Eqs. (55) - (61) clearly demonstrate that the phase-mixed AWs with $\varkappa \neq 0$ can become nonlinearly unstable at very small amplitudes, $B_k/B_0 \gtrsim 10^{-6}$. With these amplitudes, the parametric decay becomes stronger than the collisional dissipation of the phase-mixed AW, $\gamma_{NL} > \gamma_{cL}$.

5.6. Nonuniformity thresholds

We consider three effects of nonuniformity on the parametric decay of phase-mixed AW.

1. It should be noted that although the decay of the $\varkappa^2 \ll 1$ pump wave into counterstreaming KAWs is local in $k_\perp$-space, it is non-local in k_z-space because $|k_{2z}|/k_z \lesssim \varkappa^2 \ll 1$. This means that our results on this decay are applicable as long as the large parallel wavelength of the counterstreaming (decay) KAW is shorter than the inhomogeneity length scale, $|k_{2z}|^{-1} \lesssim L_\parallel$. Although our results can be used for waves with $\lambda_{2z} \sim L_\parallel$ as order of magnitude estimates, for larger wavelengths they can be significantly affected by the non-uniformity. The corresponding marginal perpendicular wavenumber of the pump wave and its parallel wavelength are related through $\varkappa^2 \sim \lambda_z/L_\parallel$.

2. Also, the efficiency of the decay including counterstreaming AWs in a nonuniform plasma may be reduced by the finite correlation length along the field lines, $L_{c\parallel}$. This correlation length may be estimated as $L_{c\parallel} \approx V_A/t_s$, where t_s is the duration of the quasi-periodic pulse that excites the pump wave. We can estimate the corresponding threshold for decay into counterstreaming KAWs from the condition that the waves should overlap during the growth time ($\gamma_k^{NL} > V_A/L_{c\parallel}$):

$$\left|\frac{B_k}{B_0}\right|_{thr} \approx 2.5\sqrt{\beta}\left(k_z\varkappa^2 L_c\right)^{-1}\frac{\omega_k}{\Omega_i}, \tag{62}$$

which can be high for the waves with short correlation lengths.

3. The progressive detuning of the perpendicular wavenumbers of the interacting AWs triplet can limit the decay if the time of the nonlinear interaction is shorter than the time required to change the wavenumbers. The physics of this process is as follows. In the course of time, the initially most effectively

interacting triplet of resonant waves is removed from its top position in the wavenumber space, because the different temporal behaviour of the constant and evolving components of the perpendicular wave vectors changes the wavenumber's ratios in the triplet. The corresponding limitation on the pump wave amplitude may be found from the condition $\gamma_{NL} > \omega/k_\perp L_A$.

6. Nonlinear damping of the phase-mixed AWs in corona

As in the Discussion, we take the length-scale of the field-aligned inhomogeneity in a coronal hole $L_\parallel \sim 10^5$ km, the transverse inhomogeneity length-scale ranging as 1 km $\lesssim L_\perp \lesssim 10^3$ km, and wave amplitudes ranging from 0.01 to 0.03 for B/B_0.

For wave frequencies $\omega > 1$ s^{-1} (see Discussion), the nonuniformity restrictions for the decay into counterstreaming waves may be satisfied. Then, using the damping rate (57) in (32), we find that the pump wave amplitude decays with height as

$$A = A_0 \times \exp\left(-\frac{z^3}{z_N^3}\right), \tag{63}$$

where the distance of nonlinear damping

$$z_N = \left[\left(0.1\omega^2 \frac{V_A^2}{\Omega_i^2} V_A^{-3} L_A^{-2}\right) \Omega_i \frac{V_{Ti}}{V_A} \left|\frac{B_k}{B_0}\right|\right]^{-1/3}. \tag{64}$$

To compare this height with the field-aligned wavelength we rewrite z_N as

$$z_N = \lambda_z \left[\frac{(2\pi)^2}{10} \frac{\rho_i \lambda_z}{L_A^2} \left|\frac{B_k}{B_0}\right|\right]^{-1/3}, \tag{65}$$

where the coefficient before λ_z strongly depends on the perpendicular nonuniformity length-scale $L_{A\perp}$.

Let us apply the above results to phase-mixed Alfvén waves in a coronal hole. Taking $\rho_i \sim 1$ m, $B_k/B_0 \sim 10^{-2}$, and $\lambda_z \sim 10^7$ m, we obtain a low damping height in the coronal holes, varying in the range from $z_N \gtrsim \lambda_z$ with $L_{A\perp} = 1$ km, up to $z_N = 10^2 \lambda_z$ with $L_{A\perp} = 10^3$ km. Note that the ion gyroradius is nevertheless very small compared to $\lambda_\perp$ at these heights.

The corresponding transverse wavelengths, $\lambda_{\perp N} = 0.7$ km with $L_{A\perp} = 1$ km and $\lambda_{\perp N} = 7$ km with $L_{A\perp} = 10^3$ km, are much longer than the dissipative length-scale, $l_d \sim 10^2$ m. This is exactly the point we made in the Introduction that the effect of FLR in Alfvén waves comes into play at length scales which are much longer than l_d.

7. Collisional dissipation versus parametric decay into counterstreaming waves

To find the linear/nonlinear damping of the AW with height, we proceed further using a WKB-ansatz (32) for the AW amplitude. The damping rate includes linear collisional damping and nonlinear damping due to parametric decay:

$$\gamma = \gamma_\nu - \gamma_k^{NL} = -0.5\nu k_\perp^2 \delta_e^2 - 0.3\Omega_i \frac{V_A}{V_{Ti}} \varkappa^2 \left|\frac{B_k}{B_0}\right|.$$

Taking integrals in the exponent we find the same behaviour of the amplitude with height as in the case of collisional damping of the phase-mixed wave, but now with the cumulative dissipation distance z_{cN}:

$$A = A_0 \times \exp\left(-\frac{z^3}{z_{cN}^3}\right), \tag{66}$$

where z_{cN} is determined by the relation

$$\frac{1}{z_{cN}^3} = \frac{1}{z_c^3}\left(1 + \frac{z_c^3}{z_N^3}\right), \tag{67}$$

and the nonlinear damping height is given by (64). The collisional damping height z_c is determined by (41), which we rewrite in the form

$$z_c = \left[\left(0.1\omega^2 \frac{V_A^2}{\Omega_i^2} V_A^{-3} L_A^{-2}\right) \nu_e \frac{m_e}{m_i}\right]^{-1/3}. \tag{68}$$

In a coronal hole it can be estimated as $z_c = \left(10^2 - 10^3\right) \times \lambda_z$, which corresponds to the transverse wavelengths $\lambda_\perp \sim 10^2$ m.

We see that the characteristic height of the wave damping, z_{cN}, can be very different from that predicted by resistive MHD, z_c, if $z_c > z_N$, which gives the condition for the nonlinearly-dominated phase-mixing:

$$\left|\frac{B_k}{B_0}\right| > \bar{B}_N = \sqrt{\frac{m_e}{m_i}} \frac{\nu_e}{\Omega_i} \frac{V_A}{V_{Te}}. \tag{69}$$

The corresponding threshold amplitude $\bar{B}_N$ does not depend on the wave parameters and is almost the same as the collisional threshold for the parametric decay itself (60), which is a consequence of the local character of the AW parametric decay in $k_\perp$-space.

If condition (69) is satisfied, the initial Alfvén waves, excited at the base of the solar corona, are damped at heights $\sim z_N$. For typical coronal hole conditions discussed above, we obtain amplitudes of AWs, leading to the nonlinearly-dominated regime of phase-mixing:

$$\left|\frac{B_k}{B_0}\right| > 10^{-6}. \tag{70}$$

If the nonthermal broadening known from the spectral observations is due to AWs, then the wave amplitudes $B_k/B_0 = 0.01 - 0.03$, and condition (70) is well satisfied. Then the damping height in this nonlinearly-dominated regime $z_{cN} \simeq z_N$.

The competition of the linear and nonlinear damping mechanisms for the phase-mixed AWs, including parametric decay into both parallel-propagating and counterstreaming waves, collisional dissipation and Landau damping, is studied in more detail in the accompanying paper (Voitenko & Goossens 2000).

8. Discussion

The results obtained in the present paper show that the process of phase-mixing, which is inevitable in the non-uniform solar corona, can switch on the parametric decay of AWs into a spectrum of secondary AWs. As a result, the waves generated at the

base of a coronal magnetic structure undergo a transition from laminar to nonlinear (or even turbulent) propagation at a height $z = z_N$, determined by the plasma and wave parameters. Consequently, the whole picture of the AW dynamics in a coronal plasma may be considerably modified, and not only at heights $z > h_c$, but also at $z < z_N$, because a part of the wave flux can reverse its direction of propagation if the time of parametric decay into counterstreaming AWs is shorter than the time of wave dissipation. The energy transferred to the inward propagating AWs will not directly contribute to accelerating the solar wind; but it can again couple nonlinearly to upward propagating waves, increasing the transverse wavenumbers.

We found that the collisional wave dissipation of the phase-mixed AW, represented by the Ohmic dissipation of the parallel wave current, is much weaker than the nonlinear damping due to parametric decay. The linear damping rate due to the ion-ion collisions (shear ion viscosity) can in some cases be comparable to Ohmic dissipation (Hasegawa & Chen 1976), but can hardly exceed it. Under coronal hole conditions $\gamma_{ei}/\gamma_{ii} \sim 10$.

In Sect. 4 our results have been applied to the phase-mixed Alfvén waves in a coronal hole. The influence of vertical inhomogeneity in coronal holes on the AW phase mixing has been investigated in great detail in the linear approximation (Ruderman et al. 1998; De Moortel et al. 1999). The nonlinear generation of fast MHD waves by phase-mixed AWs has been considered by Nakariakov et al. (1997), but this process seems to be less effective for waves with amplitudes ~ 0.01, as suggested by observations. It is therefore important to check if a nonlinear process can influence phase mixed AWs in the corona, and in coronal holes in particular.

The length-scale of the field-aligned inhomogeneity in a coronal hole is primarily determined by the characteristic scale of the density variation with height, $L_\parallel \sim h_g \sim 10^5$ km. The transverse inhomogeneity length-scale is uncertain. If $L_\perp$ is determined by the visible plume sizes, then one can take $L_\perp \sim 10^3$ km. However, it is quite possible that the corona is much more structured in the horizontal direction, up to $L_\perp \sim 1$ km (Woo 1996).

The wave frequency is also not an accurately known parameter in the problem. From the point of view of the power present in the photospheric motions, and in the magnetic fields of the chromosphere and corona, it can range from $\omega \sim 10^{-3}$ s^{-1}, for the waves excited by granular motions, up to $\omega \sim 10^6$ s^{-1}, for waves excited by the small-scale magnetic activity in the chromospheric network (Axford & McKenzie 1992). Persistent nonthermal plasma motions in the corona have been confidently detected by means of spectroscopic observations, (Saba & Strong 1991; Tu et al. 1998; Hara & Ichimoto 1999, and references therein). Wave amplitudes estimated from these data range from 0.01 to 0.03 for B/B_0, and energy requirements can be satisfied.

However, because of the lack of observational evidence that the low-frequency global modes supply the energy for the high-temperature corona, one can suppose that either the wave periods fall below the available time resolution, $\tau < 1$ s $\left(\omega \gtrsim 1\ \mathrm{s}^{-1}\right)$, or the wave coherence lengths can not yet be spatially resolved, i.e., at least, wavelength $\lambda \lesssim 10^6$ m. This last condition in turn maps onto the frequency scale as $\omega \gtrsim 1\ s^{-1}$ for Alfvén waves if λ is the parallel wavelength. In principle, Alfvén waves with $\lambda_\perp \ll 10^6$ m can be highly localized in planes perpendicular to $\mathbf{B}_0$, which makes them unresolved. But the direct footpoint excitation of short-scale waves requires too much power in the photosphere concentrated at small scales, and any alternative process involving an evolutional structurization in the corona should be observed at the initial large-scale stage if $\omega < 1\ \mathrm{s}^{-1}$.

In the closed magnetic configurations, like coronal loops, the random global photospheric motions can excite short-scale standing AWs localized around resonant field lines, where the Alfvén travel time is equal to the photospheric time-scale at which the photospheric motions contain enough energy (De Groof et al. 1998). The problem here is that the setup time seems to be long compared to $\leq$ 1-minute variations of the fine-scale chromospheric activity, repulsing the dynamics of the coronal heating process (Berger et al. 1999).

The above consideration suggests that the waves responsible for coronal heating have frequencies $\omega \gtrsim 1\ s^{-1}$, or even higher (Tu et al. 1998; Wilhelm et al. 1998). Moreover, this suggestion can help to circumvent some difficulties with in situ spacecraft observations of waves in the solar wind. Using the k^{-1} spectra derived from the Helios (and later Ulysses) observations, Roberts (1989) has shown that the wave energy contained in those spectra, is not sufficient to accelerate the solar wind when extrapolated to the corona. This difficulty can be circumvented by a spectrum of AWs with higher frequencies, which can be effectively dissipated by cyclotron damping when the waves reach the height where the cyclotron frequency equals the wave frequency (Axford & McKenzie 1992; Tu et al. 1998).

At the same time, small perpendicular length scales do often develop; they are important for AWs and open various alternative dissipation channels (Matthaeus et al. 1999; Hollweg 1999). The structurization can be very efficient for the high-frequency AWs in a nonuniform coronal plasma because they undergo strong phase mixing and quickly develop strong transverse gradients that accelerate the nonlinear interaction. Nonlinear decay initially spreads the input wave spectrum out over short wavelengths across the magnetic field as shown on Figs. 2 and 3, and over long wavelength in parallel direction (not shown). With sufficient driver power, a further growth of the secondary waves gives rise to the nonlinear coupling among them resulting in the anisotropic turbulent cascade.

Another possible scenario is that anisotropic turbulent cascade is excited by the parametric instability of parallel-propagating AW (Ghosh & Goldstein 1994). Note that our approach differs from that in the papers (Viñas & Goldstein 1991; Ghosh et al. 1993; Ghosh & Goldstein 1994) in both the physical model and the origin of nonlinearity involved. While it is quite natural to take the parallel dispersion for the parallel-propagating waves into account (Viñas & Goldstein 1991), it is equally natural that the perpendicular dispersion is important for the highly oblique Alfvén wave. The planar model used in the above papers restricts all waves to propagate in the $(x - z)$

plane. Since our leading nonlinearity contains the vector product of perpendicular wave vectors, the $2\frac{1}{2}$ D simulations reduce it to zero and hence can not account for it. Also, the use of one-fluid or reduced two-fluid equations rules out important nonlinear couplings of oblique AWs. This happens, in particular, when the nonlinear terms due to electron and ion electric drifts are assumed to be cancelled by each other.

It is not certain presently if the nonlinear interaction of AWs alone can reproduce the one-dimensional power $\mathbf{k}^{-1}$ spectra with most (80%) fluctuation energy hidden in the small-scale transverse spectra as suggested by observations of the solar wind (Matthaeus et al. 1999 and references therein). The analysis of possible causes of the appearance of anisotropic spectra suggests (Ghosh et al. 1998) that their most probable source is in the solar corona, where the solar wind originates. The anisotropic spectra can indeed be developed in the corona by the wave-wave interactions that we study, but with an even flatter parallel power spectral index $-1/2$ (the perpendicular power index is -2) (Voitenko 1998b). Such a flat spectrum can steepen towards an index -1 by the Landau damping which has a $\sim k_z$ dependence on the parallel wave number, but exact final spectra can be obtained via numerical simulations.

The dynamics of the spectrum of parallel-propagating AWs has been discussed by Agim et al. (1995) for waves generated by a proton beam. On the contrary, our input phase mixed spectra are essentially anisotropic. For example, if the initial one-dimensional spectrum of AWs is $\sim k_z^{-1/2}$ at the base of corona, the two-dimensional spectrum created by phase mixing is $\sim k_z^{-1/2}k_x^{-1/2}$, x is in the direction of inhomogeneity. This spectrum is restricted to the $(z-x)$ plane and is thus parametrically unstable in the sense we are discussing, exciting waves with $k_y \neq 0$. This is a feature of the vector nonlinearity ($\sim (k_1 \times k_2)_z$), involving waves propagating in the different directions across $\mathbf{B}_0$.

As we restricted our analysis to the wavelengths λ_z shorter than the vertical inhomogeneity length-scale, $L_\parallel \sim 10^5$ km, $\omega \gtrsim 10^{-2}$ s^{-1}. Also, the competition of the parametric decay into counterstreaming waves with collisional dissipation may be reduced in the low-frequency range, $10^{-2}\ s^{-1} < \omega < 10$ s^{-1}, where this decay channel is prohibited by the field-aligned plasma inhomogeneity and decay into parallel-propagating waves comes into play (see Voitenko & Goossens 2000). Although, as we discussed above, this low-frequency range tends to be excluded from the observational point of view, the corresponding linear and nonlinear wave damping is considered by Voitenko & Goossens (2000).

Here we neglected kinetic damping effects in comparison to collisional dissipation. To describe the dissipation of high frequency AWs, one has, in principle, to use the kinetic plasma model, accounting for the Landau damping. However, noting that the two-fluid MHD dispersion of AWs is close to the exact kinetic dispersion in the whole range of perpendicular wavenumbers and frequencies, one can use the two-fluid MHD model with the semi-empirically included Landau damping for the high-frequency AWs also. Moreover, the Landau damping itself may be reduced by the quasilinear relaxation of the velocity-space distribution, in which case the competition of the damping due to collisions and decay into counterstreaming waves can extend into high-frequency region, up to $\omega \lesssim 10^6$ s^{-1}.

The complicated interplay of the different damping mechanisms in the different frequency ranges is studied by Voitenko & Goossens (2000).

9. Conclusions

The main conclusions of the present paper are:

1. Phase mixing of finite-amplitude Alfvén waves in the corona gives rise to nonlinear coupling of AWs and to spectral energy redistribution. The strongest coupling in the plasma, which is uniform along $\mathbf{B}_0$, includes counter-propagating waves.
2. The nonlinear effects of a non-zero ion Larmor radius on the finite-amplitude Alfvén waves comes into play at length scales which are much longer than the dissipation length-scale l_d. In the coronal holes, the phase-mixing switches to the nonlinear phase at the heights equal to $10-100$ parallel wavelengths λ_z, where the transverse wavelength $\lambda_\perp \sim 10^4$ m while the dissipation length-scale is $l_d \sim 10^2$ m.
3. Nonlinear coupling introduces a spectral redistribution of the wave energy, thus changing the rate of the dissipation of wave flux. The influence of the nonlinear interaction on the actual dissipation of the wave flux and consequent plasma heating depends on the frequency of the waves and is a subject of further investigations. The part of wave energy which is transferred to smaller scales can be damped rapidly by collisional dissipation.
4. The distance at which the phase-mixing undergoes a transition from a laminar to a nonlinear stage depends on the wave frequency and amplitude. In the case of the decay into counterstreaming waves this distance is proportional to $\omega^{-2/3}\left(B_k/B_0\right)^{-1/3}$ and is given by (64).

Acknowledgements. This work was supported by the FWO-Vlaanderen grant G.0335.98 and by Intas grant 96-530. Yu.V. acknowledges the financial support by the KUL and by Ukrainian FFR grant 2.4/1003.

References

Agim Y.Z., Viñas A.F., Goldstein M.L., 1995, J. Geophys. Res. 100 (A9), 17, 081

Axford W.I., McKenzie J.F., 1992, In: Marsch E., Schwenn R. (eds.) Solar Wind Seven. Pergamon Press, Oxford, England, p. 1

Berger T.E., De Pontieu B., Schrijver C.J., Title A.M., 1999, ApJ 519, 97

Bodo G., Ferrari A., 1982, A&A 114, 394

de Azevedo C.A. Elfimov A.G., de Assis A.S., 1994, Solar Phys. 153, 205

De Groof A., Tirry W., Goossens M., 1998, A&A 335, 329

De Moortel I., Hood A.W., Ireland J., Arber T.D., 1999, A&A 346, 641

Elfimov A.G., de Azevedo C.A., de Assis A.S., 1996, Physica Scripta T63, 251

Erokhin N.S., Moiseev S.S., Mukhin V.V., 1978, Sov. Phys. Plasma 4, 1172 (in Russian)
Galeev A.A., Sagdeev R.Z., 1979, In: Leontovich M.A. (ed.) Reviews of Plasma Physics Vol. 7, Plenum, New York, p. 1
Ghosh S., Goldstein M. L., 1994, J. Geophys. Res. 99 (A7), 13, 351
Ghosh S., Viñas A.F., Goldstein M.L., 1993, J. Geophys. Res. 98 (A9), 15, 561
Ghosh S., Matthaeus W.H., Roberts D.A., Goldstein M.L., 1998, J. Geophys. Res. 103 (A10), 23, 705
Goldstein M.L., 1978, ApJ 219, 700
Goossens M., 1994, Space Sci. Rev. 68, 51
Hara H., Ichimoto K., 1999, ApJ 513, 969
Hasegawa A., Chen L., 1976, Phys. Fluids 19, 1924
Hasegawa, A., Chen, L., 1992, Ann. Geophysicae 10, 644
Heyvaerts J., Priest E.R., 1983, A&A 117, 220
Hollweg J.V., 1999, J. Geophys. Res. 104 (A7), 14, 811
Hood A.W., Ireland J., Priest E.R., 1997a, A&A 318, 957
Hood A.W., Gonzalez-Delgado D., Ireland J., 1997b, A&A 324, 11
Jaun A., Hellsten T., Appert K., et al., 1997, Plasma Phys. Contr. Fusion 39, 549
Jayanti V., Hollweg J.V., 1993, J. Geophys. Res. 98 (A7), 13, 247
Matthaeus W.H., Zank G.P., Leamon R.J., Smith C.W., Mullan D.J., 1999, Space Sci. Rev. 87, 269
Nakariakov V.M., Roberts B., Muravski K., 1997, Solar Phys. 175, 93
Ofman L., Davila J.M., 1995, J. Geophys. Res. 100 (A12), 23,413
Ofman L., Davila J.M., 1997, ApJ 476, 357
Poedts S., Goedbloed J.P., 1997, A&A 321, 935
Roberts D.A., 1989, J. Geophys. Res. 94 (A6), 6899
Ruderman M.S., Nakariakov V.M., Roberts B., 1998, A&A 338, 1118
Ruderman M.S., Goldstein M.L., Roberts D.A., Deane A., Ofman L., 1999, J. Geophys. Res. 104 (A8), 17, 057
Ryutova M.P., Habbal S.R., 1995, ApJ 451, 381
Saba J.L.R., Strong K.T., 1991, ApJ 375, 789
Shukla P.K., Murtaza G., Yu M.Y., 1989, Phys. Fluids B1, 702
Shukla P.K., Stenflo L., 1995, Physica Scripta T60, 32
Tu C.-Y., Marsch E., Wilhelm K., Curdt W., 1998, ApJ 503, 475
Viñas A.F., Goldstein M.L., 1991, J. Plasma Phys. 46, 129
Voitenko Yu.M., 1994, In: Space plasma physics. NSAU, Kiev, p. 221
Voitenko Yu.M., 1995, Solar Phys. 161, 197
Voitenko Yu.M., 1996a, Solar Phys. 168, 219
Voitenko Yu.M., 1996b, In: Bentley R.D., Mariska J.T. (eds.) Magnetic reconnection in the solar atmosphere. ASP Conference Series 111, p. 312
Voitenko Yu.M., 1996c, In: Gressilon D., Sitenko A., Zagorodny A. (eds.) Controlled Fusion and Plasma Phys. ECA Series 20C, Part III, p. 1293
Voitenko Yu.M., 1998a, J. Plasma Phys. 60, 497
Voitenko Yu.M., 1998b, J. Plasma Phys. 60, 515
Voitenko Yu.M., 1998c, Solar Phys. 182, 411
Voitenko Yu.M., Kryshtal A.H., Malovichko P.P., Yukhimuk A.K., 1990, Geomagnetism and Aeronomy 30, 402
Voitenko Yu.M., Goossens M. 2000, A&A accepted
Volokitin A.S., Dubinin E.M., 1989, Planet. Space Sci. 37, 761
Wilhelm K., Marsch E., Dwivedi B.N., et al., 1998, ApJ 500, 1023
Woo R., 1996, Nat 379, 321
Yukhimuk A.K., Kucherenko B.P., 1993, Kinem. Phys. Celest. Bodies. 9(3), 33
Yukhimuk A.K., Sirenko E.K., Yukhimuk V.A., Voitenko Yu.M., 1999, Odessa Astronomical Publications 12, in press